Yb^{3+} f-f excitations in $NaYbSe_2$: Benchmarking embedded-cluster quantum chemical schemes for $4f$ insulators

P. Bhattacharyya and L. Hozoi
Institute for Theoretical Solid State Physics, Leibniz IFW Dresden, Helmholtzstrasse 20, 01069 Dresden, Germany

(Received 23 March 2022; revised 12 May 2022; accepted 6 June 2022; published 15 June 2022)

$\tilde{S} = 1/2$ triangular-lattice f-electron materials define a dynamic research area in condensed matter magnetism. In various Yb $4f^{13}$ triangular-lattice compounds, for example, spin-liquid ground states seem to be realized. Using *ab initio* quantum chemical methods, we here investigate how correlation effects involving the $4f$ electrons affect the on-site f-f excitation spectrum in $NaYbSe_2$. The system is well suited for such a study since unambiguous inelastic neutron scattering data are available for the Yb^{3+} f-f transitions. The excitation energies obtained by configuration-interaction calculations with single and double substitutions agree within 3–4 meV with experimental values, which provides a not so expensive alternative to fitting experimental data at the model-Hamiltonian level in order to analyze f-center multiplet structures.

DOI: 10.1103/PhysRevB.105.235117

I. INTRODUCTION

Triangular-lattice rare-earth (R) delafossites with the general formula ARX_2 provide an appealing platform for investigating frustrated quantum magnetism, in particular, the possibility of realizing quantum spin-liquid ground states [1,2]. Aside from geometrical frustration, the strong $4f$-shell spin-orbit coupling (SOC) and edge-sharing arrangement of adjacent RX_6 octahedra leave room for large intersite exchange anisotropy and additional frustration [2,3]. From an electronic-structure point of view, the simplest $4f$-shell electron configurations are in principle $4f^1$ and $4f^{13}$, with either one electron or one hole within the set of seven $4f$ orbitals. Such $4f$-shell occupations are realized in, e.g., $KCeX_2$ and $NaYbX_2$ compounds, where X can be O, S, or Se. Since $S = 1/2$ and $L = 2$, SOC yields $J = 7/2$ and $J = 5/2$ terms, split up in solids due to crystal-field effects. The $J = 5/2$-like states describe the low-energy multiplet structure of Ce^{3+} ions in $KCeX_2$ delafossites, while the relevant low-energy states for Yb^{3+} are related to the free-ion $J = 7/2$ term. In lower symmetries (e.g., D_{3d} $4f$-site symmetry in ARX_2 delafossites), the $J = 5/2$-like spectrum amounts to three Kramers doublets, i.e., two low-energy on-site excitations. Interestingly, three high-intensity peaks have been found experimentally in $KCeS_2$ [4], $KCeO_2$ [5], and $RbCeX_2$ (X = O, S, Se, and Te) [6], which indicates additional degrees of freedom in the Ce-based delafossites, presumably strong vibrational couplings. On the other hand, one excitation is missed in the inelastic neutron scattering (INS) measurements on $NaYbS_2$ [7]. While *ab initio* quantum chemical methods were in those cases helpful in achieving a more complete picture of the underlying multiplet structures [4,7], in order to test in greater detail the abilities of quantum chemical computational schemes, it is desirable to use as reference safer sets of experimental data. This seems to be achieved in $NaYbSe_2$, for which convergent INS results have been reported for the expected three low-energy excited-state $4f^{13}$ terms [8,9]. Here we address the $4f^{13}$ electronic structure of $NaYbSe_2$ by quantum chemical methods and evidence that correlation effects are important. In particular, it is shown that a rather advanced type of correlation treatment is required in order to achieve reasonable agreement with experiment for the f-f excitation energies. The analysis provides useful reference computational data in the context of correlation effects in $4f$-electron insulators, which have been much less investigated by *ab initio* quantum chemical techniques in comparison to d-electron compounds.

II. COMPUTATIONAL DETAILS

Trigonally distorted, edge-sharing $YbSe_6$ octahedra decorate a two-dimensional triangular magnetic lattice in $NaYbSe_2$, as presented in Fig. 1(a). To achieve a correct picture of the Yb^{3+} $4f^{13}$ multiplet structure in this crystalline environment, quantum chemical calculations were carried out using the MOLPRO [11] computer program; in these computations, a finite cluster composed of a $YbSe_6$ octahedron, six adjacent Yb sites, and 12 Na nearest neighbors was considered, as shown in Fig. 1(b). This finite fragment was embedded within a large array of point charges, which replicate the crystalline Madelung field[1] within the cluster region; this distribution of point charges was generated using the EWALD package [12,13]. We employed a similar material model with simple point-charge embedding [14] to study the Ce^{3+} $4f^1$ multiplet structure in $NaCeO_2$ and found excellent agreement between experimental results and our computed f-f excitation energies and g factors; this convincing confirmation of the material model motivated us to apply a similar methodology for investigating the Yb^{3+} $4f^{13}$ multiplet

[1]A fully ionic picture was assumed, with formal charges of +1, +3, and −2 at the Na, Yb, and Se sites, respectively.

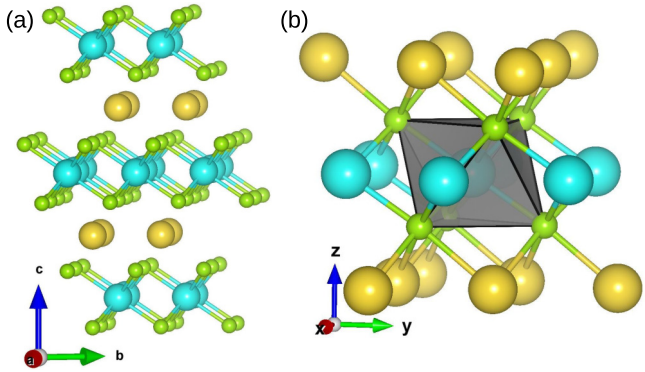

FIG. 1. (a) Crystal structure of $NaYbSe_2$ with successive ionic layers, plotted using the VESTA visualization program [10]. (b) Finite cluster considered in the computations. Cyan, yellow, and green spheres denote Yb, Na, and Se sites, respectively.

structure in the $NaYbSe_2$ compound. More sophisticated embedding schemes are based on, e.g., density functional theory [15–17] or prior Hartree-Fock computations for the periodic system [18,19].

The quantum chemical study was initiated as complete active space self-consistent field (CASSCF) calculations [20,21]. For this purpose, an active orbital space containing the seven $4f$ orbitals of the central Yb atom was considered. We obtained the seven crystal-field states related to the $4f^{13}$ manifold using a state-averaged variational optimization [20]. Next we performed electron-correlated computations at the level of multireference configuration interaction (MRCI) with single and double excitations (MRSDCI) [20,22] out of the Yb $4f$ and Se $4p$ orbitals of the central $YbSe_6$ octahedron. Finally, we carried out spin-orbit calculations following the procedure described in Ref. [23]. The diagonal elements of the spin-orbit matrix in the final MRCI+SOC step were replaced by Davidson-corrected [20] MRCI energies to obtain the results enlisted in the fifth column of Table I. In these computations, for the central Yb ion quasirelativistic pseudopotentials [25] and valence basis sets of quadruple-ζ quality [26,27] were employed, whereas we used all-electron triple-ζ basis sets for the Se ligands of the central $YbSe_6$ octahedron [28]. Large-core pseudopotentials were adopted for the six Yb nearest neighbors [29] and also for the 12 adjacent Na cations [30]. For the former, the $4f$ electrons are also part of the effective potential.

Crystallographic data were used as provided in Ref. [31]. $NaYbSe_2$ exhibits an $R\bar{3}m$ layered structure (space-group number 166) [32] (see Fig. 1); the Wyckoff positions of Na, Yb, and Se are 3a (0,0,0), 3b (0, 0, 1/2), and 6c (0,0,0.2424), respectively, whereas the experimentally determined lattice constants are $a = b = 4.0568$ Å and $c = 20.7720$ Å [31]. A given $YbSe_6$ octahedron features D_{3d} point-group symmetry, with Yb-Se bond lengths of 2.82 Å and as a result of trigonal compression Se-Yb-Se bond angles of 88.07° and 91.93°.

III. RESULTS AND DISCUSSION

Results obtained from CASSCF and MRCI computations without and with spin-orbit coupling are provided in Table I, along with INS data. Without SOC, one A_{1u}, two nondegenerate A_{2u}, and two sets of doubly degenerate E_u sublevels are expected in D_{3d} symmetry [33], out of which the $^2A_{2u}$ crystal-field state is found to be the lowest in our calculations. Though SOC defines a dominant energy scale, the sequence of the above-mentioned crystal-field levels and the magnitude of the crystal-field splittings determine the precise nature of the spin-orbit ground state. Additionally, the details of the multiplet structure depend on intra-atomic electronic correlations and to a smaller extent on R f–X p correlation effects.

The computational data summarized in Table I show that the MRCI treatment gives rise to significant corrections, of up to 35%, on top of the CASSCF approximation. A post-CASSCF correlation treatment is therefore worthy of late rare-earth ions, an aspect previously pointed out in, e.g., Refs. [34,35]. The low-lying excitation energies obtained by spin-orbit MRCI are 12.3, 20.7, and 34.6 meV. Experimentally, on-site f-f transitions are observed at 15.8, 24.3, and 30.5 meV in the INS spectrum [8]. Comparing the two sets of relative energies, we see that the MRCI+SOC results reproduce the experimental values within 10%–20%. Multireference configuration-interaction results of similar quality were obtained for the on-site multiplet structures in d-electron compounds with one single hole within the valence shell, i.e., cuprates [36,37]. It turns out that spin-orbit interactions may be sizable also in those materials [36].

Not only $NaYbSe_2$ [38,39], but also $NaYbO_2$ [40,41], $NaYbS_2$ [7], $KYbSe_2$ [42], and $RbYbSe_2$ [42] seem to realize spin-liquid ground states as no long-range order is observed at subkelvin temperatures in any of these magnetic systems. Inelastic neutron scattering data are not available for $KYbSe_2$ and $RbYbSe_2$, while in $NaYbS_2$ one f-f excitation

TABLE I. Yb^{3+} $4f^{13}$ multiplet structure in $NaYbSe_2$, with relative energies in meV. The notation corresponding to D_{3d} point-group symmetry is employed for the crystal-field (SOC not considered) and spin-orbit states (+SOC). For the double group, the notation as in Ref. [24] (e.g., Appendix I in [24]) is used. Davidson corrections [20] were added to the MRCI energies. The INS measurements are from [8].

Crystal-field states	CASSCF	MRCI	CASSCF + SOC	MRCI + SOC	INS	Spin-orbit states
$^2A_{2u}$	0	0	0	0	0	Γ_6
^2E_u	8	10	8.0	12.3	15.8	Γ_6
^2E_u	8	10	15.8	20.7	24.3	$\Gamma_4 + \Gamma_5$
$^2A_{1u}$	18	28	25.4	34.6	30.5	Γ_6
^2E_u	28	37	1275.6	1301.3		Γ_6
^2E_u	28	37	1280.5	1306.6		$\Gamma_4 + \Gamma_5$
$^2A_{2u}$	34	47	1296.2	1328.5		Γ_6

TABLE II. Ground-state g factors in $NaYbSe_2$ as obtained by CASSCF + SOC, MRCI + SOC, and electron spin resonance measurements.

g factor	CASSCF + SOC	MRCI + SOC	ESR
g_{ab}	3.25	3.19	3.13,[a] 3.10[b]
g_c	0.21	0.76	1.01,[a] 0.96[b]

[a]From Ref. [39].
[b]From Ref. [44].

is, for unclear reasons, missing in existent INS spectra [7]. Within the $NaYbX_2$ series, the lowest three f-f excitation energies are reduced in $NaYbSe_2$ compared to $NaYbO_2$ and $NaYbS_2$ [43]. This feature can be understood on the basis of the larger ligand ionic radius and increased Yb-ligand bond lengths in $NaYbSe_2$. Longer Yb-ligand bonds result in smaller ligand-field effects, i.e., weaker splittings within the $J = 7/2$ manifold. Other crystallographic/electrostatic features affecting the $4f$-shell multiplet structure are the trigonal compression of the YbX_6 octahedra and anisotropies related to the layered lattice configuration. How such effects may compete with each other was recently analyzed in, e.g., Refs. [32,43].

Yb-ion g factors computed on the basis of the spin-orbit CASSCF and MRCI wave functions are displayed in Table II, along with g factors derived by electron spin resonance (ESR) measurements [39,44] and fitting INS peak positions [8]. It can be seen that the g factors are strongly anisotropic, similar to the g factors obtained from ESR measurements on $CsYbSe_2$ [45], $NaYbS_2$ [7], and $NaYbO_2$ [40,41]. The MRCI treatment yields a very large correction to the perpendicular component g_c in particular and provides a value that is much closer to the experimental result. Remaining differences between computational and experimental results may be related to correlation effects not accounted for at the MRSDCI level but also to vibronic couplings [46–48]. Important vibronic effects were recently evidenced in the Raman spectra of both $NaYbSe_2$ [49] and $CsYbSe_2$ [50].

IV. CONCLUSION AND OUTLOOK

The performance of an embedded-cluster MRSDCI computational scheme was documented for the case of a Yb^{3+} $4f^{13}$ compound, $NaYbSe_2$. The material is part of the $AYbX_2$ delafossite family, of substantial interest in current research as a platform for quantum spin-liquid states. It represents a good testing ground for electronic-structure methods because complete, convergent INS data are available for the low-energy on-site f-f transitions [8,9]. While the reliability of the embedding scheme itself was recently proven on Ce^{3+} $4f^1$ compounds such as $KCeO_2$ [5,32] and $NaCeO_2$ [14], we focused in the present investigation on the extent of electronic correlations on an RX_6 octahedron. While minor for the Ce^{3+} $4f^1$ octahedral system [14,32], with "minimal" $4f$-shell occupation, it was shown that correlation effects are important for the Yb^{3+} $4f^{13}$ valence configuration: The MRSDCI treatment brings corrections of up to 35% to the CASSCF on-site f-f excitation energies, delivering results within 3–4 meV of experimentally determined peak positions. A sizable correlation-induced correction was also found for one of the ground-state g factors. Extensions toward the computation of full INS spectra (i.e., not only excitation energies but also intensities) for single-site scattering would provide a very effective *ab initio* tool for the analysis and interpretation of f-ion multiplet structures in lanthanide/actinide magnetic insulators.

ACKNOWLEDGMENTS

We thank T. Petersen, M. S. Eldeeb, H. Stoll, and U. K. Rößler for discussions, U. Nitzsche for technical assistance, and the German Research Foundation (Project No. 441216021) for financial support.

[1] W. Liu, Z. Zhang, J. Ji, Y. Liu, J. Li, H. Lei, and Q. Zhang, Chin. Phys. Lett. **35**, 117501 (2018).
[2] Y. Li, P. Gegenwart, and A. A. Tsirlin, J. Phys.: Condens. Matter **32**, 224004 (2020).
[3] Y. Motome, R. Sano, S. Jang, Y. Sugita, and Y. Kato, J. Phys.: Condens. Matter **32**, 404001 (2020).
[4] G. Bastien, B. Rubrecht, E. Haeussler, P. Schlender, Z. Zangeneh, S. Avdoshenko, R. Sarkar, A. Alfonsov, S. Luther, Y. A. Onykiienko, H. C. Walker, H. Kühne, V. Grinenko, Z. Guguchia, V. Kataev, H.-H. Klauss, L. Hozoi, J. van den Brink, D. S. Inosov, B. Büchner, A. U. B. Wolter, and T. Doert, SciPost Phys. **9**, 041 (2020).
[5] M. M. Bordelon, X. Wang, D. M. Pajerowski, A. Banerjee, M. Sherwin, C. M. Brown, M. S. Eldeeb, T. Petersen, L. Hozoi, U. K. Rößler, M. Mourigal, and S. D. Wilson, Phys. Rev. B **104**, 094421 (2021).
[6] B. R. Ortizy, M. M. Bordelon, P. Bhattacharyya, G. Pokharel, P. M. Sarte, L. Posthuma, T. Petersen, M. S. Eldeeb, G. E. Granroth, C. R. D. Cruz, S. Calder, D. L. Abernathy, L. Hozoi, and S. D. Wilson, arXiv:2204.12086.
[7] M. Baenitz, P. Schlender, J. Sichelschmidt, Y. A. Onykiienko, Z. Zangeneh, K. M. Ranjith, R. Sarkar, L. Hozoi, H. C. Walker, J.-C. Orain, H. Yasuoka, J. van den Brink, H. H. Klauss, D. S. Inosov, and T. Doert, Phys. Rev. B **98**, 220409(R) (2018).
[8] Z. Zhang, X. Ma, J. Li, G. Wang, D. T. Adroja, T. P. Perring, W. Liu, F. Jin, J. Ji, Y. Wang, Y. Kamiya, X. Wang, J. Ma, and Q. Zhang, Phys. Rev. B **103**, 035144 (2021).
[9] P.-L. Dai, G. Zhang, Y. Xie, C. Duan, Y. Gao, Z. Zhu, E. Feng, Z. Tao, C.-L. Huang, H. Cao, A. Podlesnyak, G. E. Granroth, M. S. Everett, J. C. Neuefeind, D. Voneshen, S. Wang, G. Tan, E. Morosan, X. Wang, H.-Q. Lin, L. Shu, G. Chen, Y. Guo, X. Lu, and P. Dai, Phys. Rev. X **11**, 021044 (2021).
[10] K. Momma and F. Izumi, J. Appl. Crystallogr. **44**, 1272 (2011).
[11] H.-J. Werner, P. J. Knowles, G. Knizia, F. R. Manby, and M. Schütz, WIREs Comput. Mol. Sci. **2**, 242 (2012).
[12] M. Klintenberg, S. Derenzo, and M. Weber, Comput. Phys. Commun. **131**, 120 (2000).
[13] S. E. Derenzo, M. K. Klintenberg, and M. J. Weber, J. Chem. Phys. **112**, 2074 (2000).

[14] P. Bhattacharyya, U. K. Rößler, and L. Hozoi, Phys. Rev. B **105**, 115136 (2022).
[15] T. Klüner, N. Govind, Y. A. Wang, and E. A. Carter, J. Chem. Phys. **116**, 42 (2002).
[16] A. S. P. Gomes, C. R. Jacob, and L. Visscher, Phys. Chem. Chem. Phys. **10**, 5353 (2008).
[17] M. Zbiri, M. Atanasov, C. Daul, J. M. Garcia-Lastra, and T. A. Wesolowski, Chem. Phys. Lett. **397**, 441 (2004).
[18] E. M. Christlmaier, D. Kats, A. Alavi, and D. Usvyat, J. Chem. Phys. **156**, 154107 (2022).
[19] L. Hozoi, U. Birkenheuer, H. Stoll, and P. Fulde, New J. Phys. **11**, 023023 (2009).
[20] T. Helgaker, P. Jørgensen, and J. Olsen, *Molecular Electronic Structure Theory* (Wiley, Chichester, 2000).
[21] D. A. Kreplin, P. J. Knowles, and H.-J. Werner, J. Chem. Phys. **152**, 074102 (2020).
[22] P. J. Knowles and H.-J. Werner, Theor. Chim. Acta **84**, 95 (1992).
[23] A. Berning, M. Schweizer, H.-J. Werner, P. J. Knowles, and P. Palmieri, Mol. Phys. **98**, 1823 (2000).
[24] S. Sugano, Y. Tanabe, and H. Kamimura, *Multiplets of Transition-Metal Ions in Crystals* (Academic, New York, 1970).
[25] M. Dolg, H. Stoll, and H. Preuss, J. Chem. Phys. **90**, 1730 (1989).
[26] X. Cao and M. Dolg, J. Chem. Phys. **115**, 7348 (2001).
[27] X. Cao and M. Dolg, J. Mol. Struct.: THEOCHEM **581**, 139 (2002).
[28] A. K. Wilson, D. E. Woon, K. A. Peterson, and T. H. Dunning, Jr., J. Chem. Phys. **110**, 7667 (1999).
[29] M. Dolg, H. Stoll, A. Savin, and H. Preuss, Theor. Chim. Acta **75**, 173 (1989).
[30] P. Fuentealba, H. Preuss, H. Stoll, and L. Von Szentpály, Chem. Phys. Lett. **89**, 418 (1982).
[31] A. K. Gray, B. R. Martin, and P. K. Dorhout, Z. Kristallogr. NCS **218**, 19 (2003).
[32] M. S. Eldeeb, T. Petersen, L. Hozoi, V. Yushankhai, and U. K. Rößler, Phys. Rev. Materials **4**, 124001 (2020).
[33] P. W. Atkins, M. S. Child, and C. S. G. Phillips, *Tables for Group Theory* (Oxford University Press, Oxford, 1970).
[34] L. Ungur and L. F. Chibotaru, Chem. Eur. J. **23**, 3708 (2017).
[35] N. Iwahara, L. Ungur, and L. F. Chibotaru, Phys. Rev. B **98**, 054436 (2018).
[36] R. Murugesan, M. S. Eldeeb, M. Yehia, B. Büchner, V. Kataev, O. Janson, and L. Hozoi, Phys. Rev. B **102**, 165103 (2020).
[37] H.-Y. Huang, N. A. Bogdanov, L. Siurakshina, P. Fulde, J. van den Brink, and L. Hozoi, Phys. Rev. B **84**, 235125 (2011).
[38] Z. Zhang, J. Li, M. Xie, W. Zhuo, D. T. Adroja, P. J. Baker, T. G. Perring, A. Zhang, F. Jin, J. Ji, X. Wang, J. Ma, and Q. Zhang, arXiv:2112.07199.
[39] K. M. Ranjith, S. Luther, T. Reimann, B. Schmidt, P. Schlender, J. Sichelschmidt, H. Yasuoka, A. M. Strydom, Y. Skourski, J. Wosnitza, H. Kühne, T. Doert, and M. Baenitz, Phys. Rev. B **100**, 224417 (2019).
[40] M. Bordelon, E. Kenney, T. Hogan, L. Posthuma, M. Kavand, Y. Lyu, M. Sherwin, C. Brown, M. J. Graf, L. Balents, and S. D. Wilson, Nat. Phys. **15**, 1058 (2019).
[41] K. M. Ranjith, D. Dmytriieva, S. Khim, J. Sichelschmidt, S. Luther, D. Ehlers, H. Yasuoka, J. Wosnitza, A. A. Tsirlin, H. Kühne, and M. Baenitz, Phys. Rev. B **99**, 180401(R) (2019).
[42] J. Xing, L. D. Sanjeewa, A. F. May, and A. S. Sefat, APL Mater. **9**, 111104 (2021).
[43] Z. Zangeneh, S. Avdoshenko, J. van den Brink, and L. Hozoi, Phys. Rev. B **100**, 174436 (2019).
[44] Z. Zhang, J. Li, W. Liu, Z. Zhang, J. Ji, F. Jin, R. Chen, J. Wang, X. Wang, J. Ma, and Q. Zhang, Phys. Rev. B **103**, 184419 (2021).
[45] T. Xie, J. Xing, S. E. Nikitin, S. Nishimoto, M. Brando, P. Khanenko, J. Sichelschmidt, L. D. Sanjeewa, A. S. Sefat, and A. Podlesnyak, arXiv:2106.12451.
[46] N. Iwahara, V. Vieru, L. Ungur, and L. F. Chibotaru, Phys. Rev. B **96**, 064416 (2017).
[47] H. Gerlinger and G. Schaack, Phys. Rev. B **33**, 7438 (1986).
[48] P. Thalmeier and P. Fulde, Phys. Rev. Lett. **49**, 1588 (1982).
[49] Y.-Y. Pai, C. E. Marvinney, L. Liang, G. Pokharel, J. Xing, H. Li, X. Li, M. Chilcote, M. Brahlek, L. Lindsay, H. Miao, A. S. Sefat, D. Parker, S. D. Wilson, and B. J. Lawrie, arXiv:2203.13361.
[50] Y.-Y. Pai, C. E. Marvinney, L. Liang, J. Xing, A. Scheie, A. A. Puretzky, G. B. Halász, X. Li, R. Juneja, A. S. Sefat, D. Parker, L. Lindsay, and B. J. Lawrie, J. Mater. Chem. C **10**, 4148 (2022).